On the Intermediacy of Chlorinated Alkylcobalt Complexes in the Reductive Dehalogenation of Chloroalkenes. A First-Principles Molecular Dynamics Study

Michael Bühl* and Volodymyr Golubnychiy

Max-Planck-Institut für Kohlenforschung, Kaiser-Wilhelm-Platz 1, D-45470 Mülheim an der Ruhr, Germany

Received July 24, 2007

According to constrained Car−Parrinello molecular dynamics (CPMD) simulations and thermodynamic integration, the free energy for protonation of a reduced cobaloxime PCE complex, $[Co(Hgly)_2(PCE)]^-$ (Hgly = glyoximato, PCE = tetrachloroethylene), to form the chlorinated ethylcobalt species $Co(Hgly)_2(CCl_2CCl_2H)(H_2O)$ is at least −10 kcal/mol in aqueous solution (employing the BP86 density functional), with an upper limit of ca. 18 kcal/mol for the free-energy barrier of this process. Because this activation barrier is lower than those computed previously for chloride elimination from PCE complexes (affording chlorinated vinylcobalt species), and because it had been shown computationally that chlorinated ethylcobalt complexes may decompose under formation of dechlorinated olefins (Pratt, D. A.; van der Donk, W. A. *Chem. Commun*. **2006**, 558), chlorinated ethylcobalt complexes are indeed viable and likely intermediates in the reductive dehalogenation of chlorinated olefins, as it is catalyzed, for example, by vitamin B_{12}.

1. Introduction

Reductive dehalogenation of chloroalkenes (sketched in Scheme 1) can be catalyzed by vitamin B_{12},[1] adding to the rich chemistry of this natural product.[2] Because of the strong interest in detoxification of halogenated pollutants with bio-inspired "Green Chemistry" methods, numerous studies have been directed at elucidating the mechanism of this catalytic process.[3−10]

In the presence of a stoichiometric, sacrificial reducing agent, such as Ti^{III}, cob(I)alamin (Cbl^I) is believed to be the key species in the catalytic cycle. Kinetic modeling of concerted and stepwise pathways has furnished evidence[3] that reduction of the chloroalkene follows an inner-sphere mechanism, that is, that reduction could actually take place in the coordination sphere of the metal. The successful isolation of chlorinated vinyl cobaloxime[3] and cobalamine complexes[11] would be consistent with such an inner-sphere mechanism, in the course of which these vinyl cobalt complexes could be formed as reactive intermediates. We have recently provided computational support for this possibility by locating viable transition states leading to vinyl complexes in a model system.[12] Specifically, it has been shown that a reduced cobaloxime $[Co(Hgly)_2]^-$ (**1**, Hgly = glyoximato) can add tetrachloroethylene (PCE) affording the olefin complex **2**, which can subsequently lose chloride under formation of the vinylcomplex **3** (Figure 1). The free-energy barrier for this process (via **TS23**) was computed to be 22.1 kcal/mol relative to **2** (19.7 kcal/mol relative to the base-on variant of **1**) at the BP86 level of density functional theory (DFT) including bulk solvation effects.

Recently, an alternate mechanistic pathway for the dehalogenation process has been proposed for cob(I)alamins, namely one involving chlorinated alkylcobalt complexes formed upon protonation,[10] for example, for PCE:

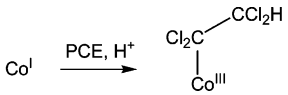

(1)

Under reductive conditions in solution, such alkyl complexes are indicated to be unstable with respect to dissociation into a Co(II) species, the dechlorinated alkene (trichloroethylene in case of eq 1), and free chloride, thereby circumventing the intermediacy of vinyl complexes.[10] For the model complexes in Figure 1, entry into this path via protonation of **2** has been computed to be strongly exergonic, with an estimated free energy in water of −30.3 kcal/mol for the reaction depicted in Figure 2.

The significance of this result was difficult to evaluate, however, because two key questions were left unanswered:

* Corresponding author. E-mail: buehl@mpi-muelheim.mpg.de.

(1) Gantzer, C. J.; Wackett, L. P. *Environ. Sci. Technol*. **1991**, *25*, 715−722.

(2) Brown, K. L. *Chem. Rev*. **2005**, *105*, 2075−2149.

(3) (a) Rich, A. E.; DeGreeff, A. D.; McNeill, K. *Chem. Commun*. **2002**, 234−235. (b) McKauley, K. M.; Wilson, S. R.; van der Donk, W. A. *Inorg. Chem*. **2002**, *41*, 393−404.

(4) (a) Lesage, S.; Brown, S.; Millar, K. *Environ. Sci. Technol*. **1998**, *32*, 2264−2272. (b) Glod, G.; Angst, W.; Hollinger, C.; Schwarzenbach, R. P. *Environ. Sci. Technol*. **1997**, *31*, 253−260. (c) Glod, G.; Brodmann, U.; Angst, W.; Hollinger, C.; Schwarzenbach, R. P. *Environ. Sci. Technol*. **1997**, *31*, 3154−3160.

(5) Costentin, C.; Robert, M.; Savéant, J.-M. *J. Am. Chem. Soc*. **2005**, *127*, 12154−12155.

(6) Burris, D. R.; Delcomyn, C. A.; Smith, M. H.; Roberts, A. L. *Environ. Sci. Technol*. **1996**, *30*, 3047−3052.

(7) For analogous dechlorination of alkyl halides, see, for example: (a) Argüello, J. E.; Costentin, C.; Griveau, S.; Saveant, J.-M. *J. Am. Chem. Soc*. **2005**, *127*, 5049−5055 and references cited therein. For a recent report on dechlorination of DDT, see: (b) Jabbar, M. A.; Shimakoshi, H.; Hisaeda, Y. *Chem. Commun*. **2007**, 1653−1655.

(8) Fritsch, J. M.; McNeill, K. *Inorg. Chem*. **2005**, *44*, 4852−4861.

(9) Follett, A. D.; McNeill, K. *J. Am. Chem. Soc*. **2005**, *127*, 844−845.

(10) Pratt, D. A.; van der Donk, W. A. *Chem. Commun*. **2006**, 558−560.

(11) (a) McKauley, K. M.; Wilson, S. R.; van der Donk, W. A. *J. Am. Chem. Soc*. **2003**, *125*, 4410−4411. (b) McKauley, K. M.; Pratt, D. A.; Wilson, S. R.; Shey, J.; Burkey, T. J.; van der Donk, W. A. *J. Am. Chem. Soc*. **2005**, *127*, 1126−1136.

(12) Bühl, M.; Vinkovic Vrèek, I.; Kabrede, H. *Organometallics* **2007**, *26*, 1494−1504.

10.1021/om7007474 CCC: $37.00
Publication on Web 10/27/2007

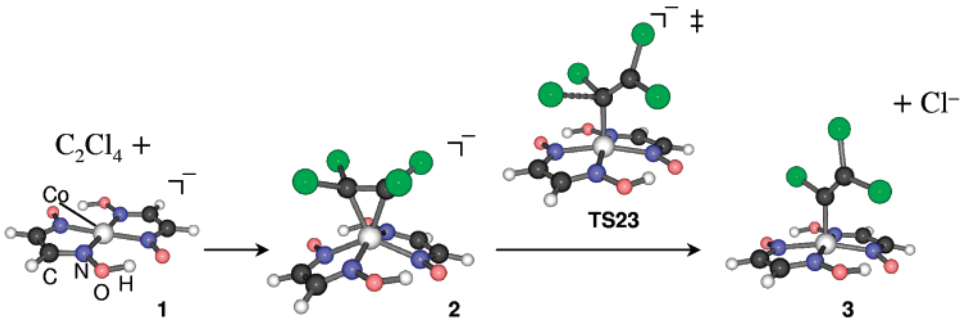

Figure 1. Key steps for PCE addition to base-off Cbl[I] model **1** and chloride elimination; BP86/AE1 stationary point from ref 12.

Scheme 1

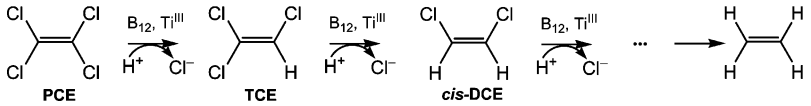

First, is the simple polarizable continuum model (PCM) employed in these calculations adequate for describing the effect of the solvent? In fact, the accurate computation of acidity constants of aqueous transition-metal complexes with this simple model is a daunting challenge.[13] Second, how large is the activation energy for this protonation step, as compared to that for the above-mentioned vinyl-complex formation? For the alkyl route to be operative, it must not only be thermodynamically favorable, but also kinetically viable.

We have now addressed these questions via constrained Car−Parrinello molecular dynamics (CPMD) simulations and thermodynamic integration including the solvent (water) explicitly. This approach has been successfully used to reproduce pK_a values of some inorganic and organic acids,[14] and recently also for metal hydrate complexes,[15] with an accuracy in the corresponding free energies of ca. 1−4 kcal/mol relative to experiment. As it turns out, there is indeed a substantial driving force for the protonation step in Figure 2, and the barrier for this step is indicated to be lower than that for the vinyl route in Figure 1.

2. Computational Details

Molecular dynamics simulations were performed using the Car−Parrinello scheme[16] as implemented in the CPMD program.[17] The BP86 combination of density functionals was used,[18,19] together with norm-conserving Troullier−Martins pseudopotentials in the Kleinman−Bylander form,[20] including the one for Co constructed and validated in ref 21. Periodic boundary conditions were imposed using cubic supercells with a box size of 13.0 Å, which contained **2** or **4a** and a total of 57 water molecules, rendering a density of 1.0. Kohn−Sham orbitals were expanded in plane waves up to a kinetic energy cutoff of 80 Ry at the Γ-point. In the dynamical simulations, a fictitious electronic mass of 600 au and a time step of 0.121 fs were used. To maintain this time step, hydrogen was substituted with deuterium. The systems were propagated for ca. 2−3 ps in the NVT ensemble using a single Nosé−Hoover thermostat set to 350 K. This somewhat elevated temperature was chosen because the BP86 functional, like many other GGAs,[22] tends to produce liquids that are too sluggish, and sometimes may even lead to a frozen rather than a liquid solution at room temperature.[15a]

For pointwise thermodynamic integration,[23] suitable reaction coordinates ξ were constructed by fixing the distances or differences of distances at successively larger or smaller values (in step sizes between 0.1 and 0.2 Å) and propagating the systems at each point until the mean force on the constraint, $\langle f(\xi)\rangle$, was sufficiently converged.[24] Helmholtz free energies[25] were then evaluated via numerical integration according to

$$\Delta A_{a\rightarrow b} = -\int_a^b \langle f(\xi)\rangle \, d\xi \qquad (2)$$

In selected cases, geometries were also fully optimized in the gas phase at the RI-BP86/AE1 level, that is, employing a fine integration grid (75 radial shells with 302 angular points per shell), the augmented Wachters' basis[26] on Co (8s7p4d, full contraction

(13) (a) Li, J., Fisher, C. L.; Chen, J. L.; Bashford, D.; Noodleman, L. *Inorg. Chem*. **1996**, *35*, 4694−4702. (b) De Abreu, H. A.; Guimaraes, L.; Duarte, H. A. *J. Phys. Chem. A* **2006**, *110*, 7713−7718.

(14) See, for example, water: (a) Trout, B. L.; Parrinello, M. *Chem. Phys. Lett.* **1998**, *288*, 343−347. (b) Sprik, M. *Chem. Phys.* **2000**, *258*, 139−150. Histidine: (c) Ivanov, I.; Klein, M. *J. Am. Chem. Soc.* **2002**, *124*, 13380−13381. Formic acid: (d) Lee, J.-G.; Asciutto, E.; Babin, V.; Sagui, C.; Darden, T.; Roland, C. *J. Phys. Chem. B* **2006**, *110*, 2325−2331.

(15) (a) Bühl, M.; Kabrede, H. *ChemPhysChem* **2006**, *7*, 2290−2293. (b) Bernasconi, L.; Baerends, E. J.; Sprik, M. *J. Phys. Chem. B* **2006**, *110*, 11444−11453.

(16) Car, R.; Parrinello, M. *Phys. Rev. Lett*. **1985**, *55*, 2471−2474.

(17) CPMD Version 3.7.0; copyright by IBM Corp. and Max-Planck-Institut für Festkörperforschung, Stuttgart, Germany.

(18) Becke, A. D. *Phys. Rev. A* **1988**, *38*, 3098−3100.

(19) (a) Perdew, J. P. *Phys. Rev. B* **1986**, *33*, 8822−8824. (b) Perdew, J. P. *Phys. Rev. B* **1986**, *34*, 7406.

(20) (a) Troullier, N.; Martins, J. L. *Phys. Rev. B* **1991**, *43*, 1993−2006. (b) Kleinman, L.; Bylander, D. M. *Phys. Rev. Lett*. **1982**, *48*, 1425−1428.

(21) Grigoleit, S.; Bühl, M. *J. Chem. Theory Comput*. **2005**, *1*, 181−193.

(22) See: VandeVondele, J.; Mohamed, F.; Krack, M.; Hutter, J.; Sprik, M.; Parrinello, M. *J. Chem. Phys.* **2005**, *122*, 014515 and references cited therein.

(23) See, for instance: Sprik, M.; Ciccotti, G. *J. Chem. Phys.* **1998**, *109*, 7737 and references cited therein.

(24) Usually within 2−3 ps after 0.5 ps of equilibration. The largest standard deviation for the running average of $\langle f(\xi)\rangle$ over the final picosecond of any point was ca. 3×10^{-4} au; multiplied with the maximal integration width of 1.1 Å, this corresponds to an estimated numerical uncertainty of ca. 0.4 kcal mol^{-1} for the derived energies. Each new point was started from the final, equilibrated configuration of the previous one. See Supporting Information for plots of the $\langle f(\xi)\rangle$ values.

(25) NVT simulations yield ΔA; because the actual volume change at constant pressure is very small, ΔA and ΔG should be very similar.

(26) (a) Wachters, A. J. H. *J. Chem. Phys.* **1970**, *52*, 1033−1036. (b) Hay, P. J. *J. Chem. Phys.* **1977**, *66*, 4377−4384.

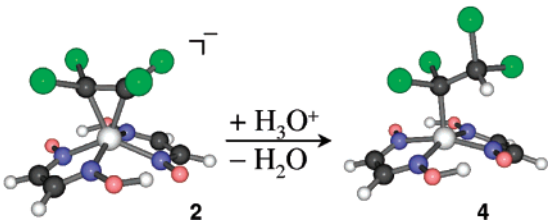

Figure 2. Protonation of **2**; BP86/AE1 minima from ref 12.

scheme 62111111/3311111/3111), 6-31G* basis[27] on all other elements, and suitable auxiliary basis sets for the fitting of the Coulomb potential.[28] This and comparable DFT levels have proven quite successful for transition-metal compounds and are well suited for the description of structures, energies, barriers, and other properties.[29,30] Harmonic frequencies were computed analytically and were used without scaling to obtain enthalpic and entropic corrections. Refined energies were obtained from single-point calculations at the RI-BP86/AE2 level, employing the RI-BP86/AE1 geometries and 6-311+G* basis[31] (instead of 6-31G*) on the non-hydrogen atoms of the ligands. With the same AE2 basis and RI-BP86/AE1 geometries, single-point energy calculations were also performed using the polarizable continuum model (PCM) of Tomasi and co-workers[32] (employing UFF radii scaled by 1.2 and the parameters of water). Energies reported at that level are denoted $\Delta E(H_2O)$. The resulting energies ΔE with AE2 basis (in vacuo or in the continuum) were corrected for the gas-phase enthalpic and entropic contributions (at the RI-BP86/AE1 level), to afford estimates for ΔG, denoted $\Delta G(H_2O)$. These computations employed the Gaussian 03 program package.[33]

3. Results and Discussion

Aqueous **2** in neutral solution remained stable for more than 3 ps in an unconstrained CPMD solution. The same was found when an additional proton was placed onto the water molecule that came closest to a C atom of the PCE ligand. Thus, if there would be a large driving force for protonation, there must be a noticeable barrier.

Chart 1

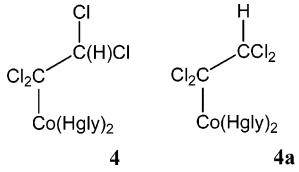

Next, the protonation product was investigated. Direct transformation of **2** into **4** with gauche orientation of the additional proton with respect to the Co−C bond would require an approach of the Brønstead acid from the same side as the glyoximato ligand. Because substantial steric hindrance is to be expected on that route, we investigated a rotamer of **4** with the additional proton anti to the Co−C bond (**4a**, Chart 1). This rotamer is the expected primary product of a backside attack of a proton on the PCE ligand in **2**. When **4a** was subjected to an unconstrained CPMD run in water, it rapidly (within 0.8 ps) attracted a water molecule from the bulk, which coordinated in trans position to the chloroalkyl group, affording $Co(Hgly)_2(CCl_2CCl_2H)(H_2O)$ (**5a**). This result is in line with the fact that alkylcobaloximes always have a donor ligand at that position. The actual protonation reaction to be studied should thus be formulated as follows:

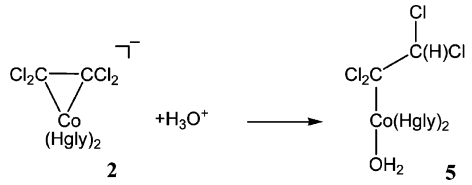

(3)

keeping in mind that **5**, the equivalent of **4** in Figure 2, will be in rapid equilibrium with **5a**:

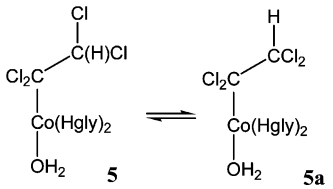

(4)

Using the same static, PCM-based approach as in ref 12, a free energy of $\Delta G_1(H_2O) = +2.0$ kcal/mol is computed in water, which should be very close to the corresponding ΔA_1 value, the Helmholtz free energy, which we will discuss from now on. Unlike for reactions of the type of eq 3, where differently charged species are involved, PCM methods are usually quite reliable for simple equilibria as in eq 4,[34] and therefore we have not investigated this rotation further and assume $\Delta A_1 = +2.0$ kcal/mol.

The protonation reaction was then studied in reverse, starting from **5a**. A path for deprotonation of **5a** was constructed by using the C−H distance r as reaction coordinate (ξ in eq 2), elongating it successively in steps of 0.1 Å (see Figure 3 for definition of the distances). With this procedure, which is analogous to that employed for other organic or inorganic acids,[14,15] the free-energy path depicted in Figure 4 was obtained.

(27) (a) Hehre, W. J.; Ditchfield, R.; Pople, J. A. *J. Chem. Phys.* **1972**, *56*, 2257−2261. (b) Hariharan, P. C.; Pople, J. A. *Theor. Chim. Acta* **1973**, *28*, 213−222.

(28) Generated automatically according to the procedure implemented in Gaussian 03.

(29) See, for instance: Koch, W.; Holthausen, M. C. *A Chemist's Guide to Density Functional Theory*; Wiley-VCH: Weinheim, 2000.

(30) In particular, as far as geometries of transition metal complexes are concerned, the popular B3LYP functional need not be superior to pure, gradient-corrected variants such as BP86, see, for instance: (a) Hamprecht, F. A. H.; Cohen, A. J.; Tozer, D. J.; Handy, N. C. *J. Chem. Phys.* **1998**, *109*, 6264−6271. (b) Barden, C. J.; Rienstra-Kiracofe, J. C.; Schaefer, H. F. *J. Chem. Phys.* **2000**, *113*, 690−700. (c) Bühl, M.; Kabrede, H. *J. Chem. Theory Comput.* **2006**, *2*, 1282−1290.

(31) (a) Krishnan, R.; Binkley, J. S.; Seeger, R.; Pople, J. A. *J. Chem. Phys.* **1980**, *72*, 650−654. (b) Clark, T.; Chandrasekhar, J.; Spitznagel, G. W.; Schleyer, P. v. R. *J. Comput. Chem.* **1983**, *4*, 294−301.

(32) As implemented in Gaussian 03: (a) Barone, V.; Cossi, M.; Tomasi, J. *J. Comput. Chem.* **1998**, *19*, 404−417. (b) Cossi, M.; Scalmani, G.; Rega, N.; Barone, V. *J. Chem. Phys.* **2002**, *117*, 43−54. (c) Cossi, M.; Crescenzi, O. *J. Chem. Phys.* **2003**, *19*, 8863−8872.

(33) Frisch, M. J.; Trucks, G. W.; Schlegel, H. B.; Scuseria, G. E.; Robb, M. A.; Cheeseman, J. R.; Montgomery, J. A., Jr.; Vreven, T.; Kudin, K. N.; Burant, J. C.; Millam, J. M.; Iyengar, S. S.; Tomasi, J.; Barone, V.; Mennucci, B.; Cossi, M.; Scalmani, G.; Rega, N.; Petersson, G. A.; Nakatsuji, H.; Hada, M.; Ehara, M.; Toyota, K.; Fukuda, R.; Hasegawa, J.; Ishida, M.; Nakajima, T.; Honda, Y.; Kitao, O.; Nakai, H.; Klene, M.; Li, X.; Knox, J. E.; Hratchian, H. P.; Cross, J. B.; Bakken, V.; Adamo, C.; Jaramillo, J.; Gomperts, R.; Stratmann, R. E.; Yazyev, O.; Austin, A. J.; Cammi, R.; Pomelli, C.; Ochterski, J. W.; Ayala, P. Y.; Morokuma, K.; Voth, G. A.; Salvafdor, P.; Dannenberg, J. J.; Zakrzewski, V. G.; Dapprich, S.; Daniels, A. D.; Strain, M. C.; Farkas, O.; Malick, D. K.; Rabuck, A. D.; Raghavachari, K.; Foresman, J. B.; Ortiz, J. V.; Cui, Q.; Baboul, A. G.; Clifford, S.; Cioslowski, J.; Stefanov, B. B.; Liu, G.; Liashenko, A.; Piskorz, P.; Komaromi, I.; Martin, R. L.; Fox, D. J.; Keith, T.; Al-Laham, M. A.; Peng, C. Y.; Nanayakkara, A.; Challacombe, M.; Gill, P. M. W.; Johnson, B.; Chen, W.; Wong, M. W.; Gonzalez, C.; Pople, J. A. *Gaussian 03*; Gaussian, Inc.: Wallingford, CT, 2004.

(34) (a) Cramer, C. J.; Truhlar, D. G. *Chem. Rev.* **1999**, *99*, 2161−2200. (b) Tomasi, J.; Mennucci, B.; Cammi, R. *Chem. Rev.* **2005**, *105*, 2999−3093.

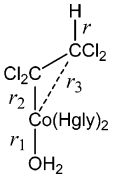

Figure 3. Definition of geometrical parameters.

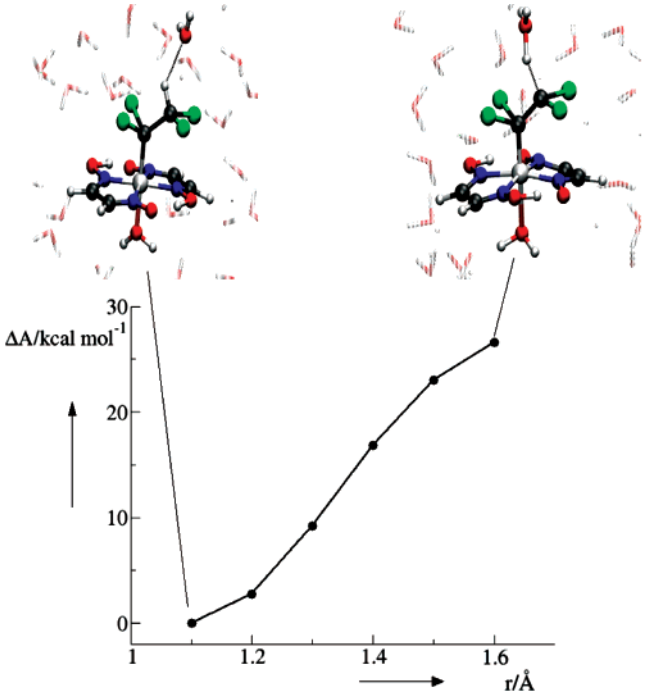

Figure 4. Change in free energy, ΔA, for deprotonation of the alkyl moiety in **5a**, as obtained from thermodynamic integration (reaction coordinate: C−H distance r, cf., Figure 3); top: representative snapshots from early and late stages of the path.

At $r = 1.7$ Å, the water ligand trans to the alkyl group detached spontaneously (within ca. 1 ps) from the metal.

For the last point where that water ligand remained coordinated, at $r = 1.6$ Å, a mean constraint force of $\langle f(r) \rangle = -0.0191$ au was obtained. This value is not yet zero, indicating that the proton transfer is not yet fully accomplished at this point. From $r = 1.3$ to 1.6 Å, the absolute value of $\langle f(r) \rangle$ shows a clear decreasing trend (cf., the value of −0.0645 au at $r = 1.3$ Å), with an additional trend toward zero during the spontaneous water detachment at $r = 1.7$ Å. The occurrence of this spontaneous process renders the chosen reaction coordinate suspect from that point on. However, only a relatively small increase in free energy would be expected if it were sensibly possible to extend the integration beyond $r = 1.6$ Å. For typical oxygen acids, for instance, an O−H distance of $r = 1.7$ Å had already turned out to be sufficient to model the fully separated species.[14,15] We thus use the free energy accumulated up to $r = 1.6$ Å as lower limit for the acidity of the alkyl complex, affording the value given in eq 5 for this quantity:

At the end of the path at $r = 1.6$ Å, the deprotonated alkyl complex **6** is present in the form of a contact ion pair with hydronium ion close to the carbanionic center.[35] Apparently, formation of the carbanion in β-position to the metal center destabilizes the bond to the *trans*-water ligand. This destabilization is apparent in a successive elongation of this Co−O(H_2) distance as r increases, from 2.10(11) Å at $r = 1.1$ Å to

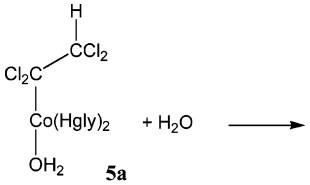

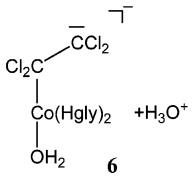

$$\Delta A_2 \geq +26.6 \text{ kcal/mol} \qquad (5)$$

2.28(16) Å at $r = 1.6$ Å (in parentheses: standard deviations during the last 1.5 ps). Together with the observation that spontaneous detachment occurs at $r = 1.7$ Å, this finding suggest only a weak binding of the water ligand at that stage and a small driving force ΔA_3 for the reaction:

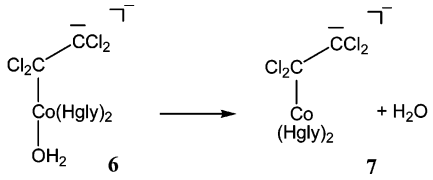

$$, \Delta A_3 \qquad (6)$$

Accurate estimation of ΔA_3 would require constrained MD simulations along an appropriate reaction coordinate, a computationally expensive procedure. For more qualitative purposes, we performed static calculations in the gas phase and in a continuum, to assess the binding energy of water to **4a** (eq 7) as a function of the C−H distance r.

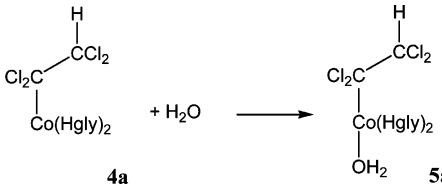

(7)

For the fully optimized minima, $\Delta E(H_2O)$ and $\Delta G(H_2O)$ values of −13.4 kcal/mol[36] and −0.3 kcal/mol, respectively, are obtained. Arguably, the entropic penalty for complex formation in bulk water will be less than suggested by the difference between these two numbers, which refer to isolated reactants (in water, the reactants would be confined in a solvent cage without full translational degrees of freedom). Thus, a substantial driving force for water binding is expected in solution, in accord with the above-mentioned unconstrained MD simulation of aqueous **4a**. When the CH distance is elongated to 1.6 and 1.7 Å,[37] the binding energy drops to $\Delta E(H_2O) = -10.0$ and −8.1 kcal/mol, respectively. This is a significant reduction, suggesting that only a very small driving force for

(35) The free energy for full separation of such a hydrated contact ion pair (or outer-sphere complex) composed of one monocation and one monoanion into the infinitely separated constituents can be estimated as $\log K = -1.12$ (based on statistical considerations of electrostatic interactions between ions in a dielectric continuum: Morel, F. M. M.; Hering, J. G. *Principles and Applications of Aquatic Chemistry*; John Wiley & Sons: New York, 1993; p 399), from which a free energy of +1.5 kcal mol^{-1} can be inferred, by which ΔA_2 in eq 5 would increase.

(36) −13.9 kcal/mol in single-point PCM energy computations employing the RI-BP86/AE1-optimized geometries, AE2 basis, and the B3LYP hybrid functional. The binding energy of water thus appears to be not very sensitive to the functional employed.

water binding will remain when entropy is taken into account.[38] We therefore assume ΔA_3 in eq 6 to be close to zero and proceed to study the transformation of **7** into **2**.

In initial constrained CPMD simulations, we tried to construct a path leading directly from **6** to **2**, by using the difference between r_3 and r_1 (see Figure 3) as coordinate, modeling an S_N2-type "backside" attack of the carbanion on the metal. To prevent reprotonation of **6**, an additional constraint was imposed on the OH bond of the hydronium ion donating a H bond to the carbanionic center. In the course of the simulations, this hydronium ion lost another of its protons to more distant water molecules, via the well-known relay mechanism of proton transport in water,[39] thus turning into a water molecule, which was not deprotonated even when this additional constraint was lifted. When the difference between r_3 and r_1 eventually was decreased stepwise from 0.9 Å (the approximate value in the simulation for deprotonated **6** with r = 1.6 Å) to 0.3 Å, both the coordinated water and the PCE ligands suddenly dissociated spontaneously, affording the Co(I) species **1**. Hence, the chosen coordinate is not suitable to attain the desired reaction product **2**.

We therefore adopted a different coordinate, using $\Delta r = r_3 - r_2$ (Figure 3) as constraint. To this end, a snapshot from the preceding path was selected, where both PCE and water were still coordinated, but the hydronium ion had wandered farther away (so that no additional constraint was necessary to prevent reprotonation). In that snapshot, Δr was fixed to 1.1 Å (the approximate value in the simulation for deprotonated **6** with r = 1.6 Å). Within 0.5 ps of constrained CPMD, the water ligand had detached, affording **7**. The simulation was continued for another 2 ps, and, subsequently, Δr was reduced to 1.0 Å, and then decreased further in steps of 0.2 Å until zero, at which point **2** was reached. To probe for possible artifacts due to hysteresis, this path was extended to negative values, including points at $\Delta r = -0.1$ to -0.7 Å (again in steps of 0.2 Å).

No significant hysteresis was encountered in this case. Integrating the mean forces from $\Delta r = 0$ to $+0.7$ Å (interpolated between the result obtained by integrating to 0.6 and 0.8 Å) and from $\Delta r = 0$ to -0.7 Å afforded free energies of 10.1 and 10.4 kcal/mol, respectively. Subsequently, the mean forces for the negative values of Δr were mapped (mirrored) onto the corresponding positive ones to have a finer mesh for the numerical integration. The resulting free-energy profile, starting from Δr = zero (i.e., complex **2**) as reference state, is depicted in Figure 5.

Starting from **2**, the free energy is constantly rising with Δr. No plateau is reached until Δr = 1.1 Å; in fact, the absolute value of $\langle f(\Delta r)\rangle$ even increases from Δr = 1.0 Å to Δr = 1.1 Å (from -0.0188 to -0.0306 au), reflected in the noticeable increase in the slope of the ΔA curve in Figure 5 between these two points. This result implies that **7** is not a stationary point

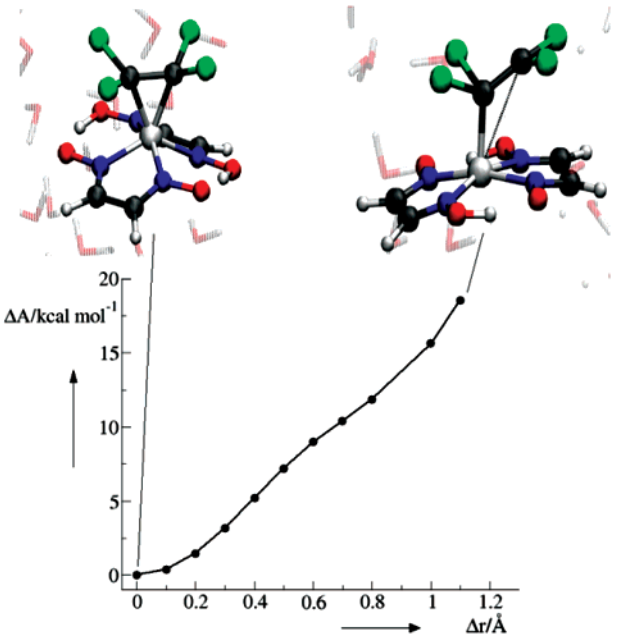

Figure 5. Change in free energy, ΔA, for ring-opening of the metallacycle in **2**, as obtained from thermodynamic integration (reaction coordinate: $\Delta r = r_3 - r_2$, cf., Figure 3); top: representative snapshots from early and late stages of the path.

on the free-energy surface. Assuming that **7** is attained when the same Δr value is reached as at the end of the path described in eq 4 (1.1 Å), the following result is obtained for ring-opening in the olefin complex:

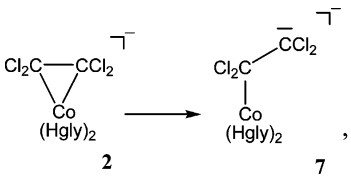

$$, \Delta A_4 = +18.5 \text{ kcal/mol} \qquad (8)$$

Taken together, eqs 3−6 and eq 8 can be viewed as thermodynamic cycle, and the overall driving force for the reaction in eq 3 can be approximated as

$$\Delta A = \Delta A_4 - \Delta A_3 - \Delta A_2 - \Delta A_1 \qquad (9)$$

affording an estimate for ΔA of ca. -10 kcal/mol. In absolute terms, this value is substantially lower than the one from the static PCM computations for the reaction in Figure 2, where $\Delta G(H_2O) \approx -30$ kcal/mol had been obtained. Both numbers are associated with substantial uncertainty, the latter due to the crude nature of the continuum model, and the former ΔA value because it is derived from imperfectly matching reaction coordinates and additional assumptions. Qualitatively, however, both computations agree that there should be a substantial driving force for this process and, hence, for the formation of alkylcobalt complexes according to eq 1. Bearing in mind that for ΔA_2 only a lower limit could be given,[35] the true ΔA value should be even more negative than the -10 kcal/mol estimate. In short, the CPMD-based approach corroborates the qualitative results from simpler, static model computations in a continuum.

What is more, however, the CPMD results can now be used to estimate an upper limit for the activation barrier of this process. In the ideal limit of fully equilibrated MD simulations for continuous reaction coordinates, the change in free energy between starting and end points of a thermodynamic integration (**2** and **5** in our case) is independent of the particular choice of

(37) For the species with elongated C−H bonds, an additional water molecule was placed explicitly near the latter H atom to model the forming H_3O^+ ion (which, in the gas-phase-optimized structures, formed two OH···Cl interactions with the Cl atoms on the α-carbon), and the two Co−C bonds were constrained to 2.1 and 3.2 Å (mean values from constrained CPMD simulations at the last point in Figure 4), to prevent any formation, full or partial, of metallacycle **2** upon removal of the water in trans position.

(38) In addition, a significant fraction of these binding energies, ca. 4 kcal/mol, is indicated to arise from basis-set superposition error (according to Counterpoise calculations, cf., Boys, S. F.; Bernardi, F. *Mol. Phys.* **1970**, *19*, 553−566), which further underscores the lability of the water ligands. It should be noted that the CPMD simulations with their periodic, plane-wave basis set do not suffer from this error.

(39) (a) Tuckerman, M. E.; Laasonen, K.; Sprik, M.; Parrinello, M. *J. Chem. Phys.* **1995**, *103*, 150−161. (b) Marx, D.; Tuckerman, M. E.; Hutter, J.; Parrinello, M. *Nature* **1999**, *397*, 601−604.

the path. This is the underlying assumption made in setting up a thermodynamic cycle and summing up the individual increments to ΔA (eq 9). Because the chosen coordinate(s) do not necessarily describe the minimum energy reaction path (and rarely do), the highest point on the chosen path is not necessarily the true transition state. The energy of this highest point, however, is an upper limit for the true barrier. In our case, this highest point is **7**, with a free energy relative to **2** of $\Delta A_4 =$ 18.5 kcal/mol (eq 8). This value implies breaking of the metal−olefin bond up to a value of $\Delta r = 1.1$ Å (see above). In practice, protonation of **7** can also occur in less distorted structures. If it would already occur at a value of, for example, $\Delta r = 1.0$ Å, the free energy up to that point would only have risen by 15.6 kcal/mol.

Even the value of ΔA_4, the upper limit, is noticeably lower than the barrier for vinylcobalt-complex formation from **2**, $\Delta G(H_2O) = 22.1$ kcal/mol,[12] from static PCM computations. Hence, the protonation route in eq 1 should not only be thermodynamically, but also kinetically favored over vinyl complex formation as in Figure 1. These findings serve to corroborate the mechanistic proposal put forward in ref 10. If our results for the cobaloxime model are transferable to cobalamins and vitamin B_{12} itself, important implications arise for the mechanism of reductive dehalogenation catalyzed by this enzyme. In that system, which contains a base tethered to the macrocyclic ligand, equilibria between "base-on" and "base-off" variants[40] (in analogy to eq 6, where water is the base) may also come into play. Further studies along these lines should be rewarding.

(40) Base-off intermediates are frequently invoked for reactive intermediates believed to be central to the chemistry of the cofactor, see, for example: Lexa, D.; Saveant, J.-M. *Acc. Chem. Res.* **1983**, *16*, 235−243.

4. Conclusions

We have provided the first computational evidence from constrained CPMD simulations and thermodynamic integration that a chlorinated alkyl cobaloxime complex can indeed be formed from a reduced Co(I) species and PCE under acidic conditions, corroborating and refining earlier results from static computations with a simple polarizable continuum. It turns out that formation of this alkyl complex is both kinetically and thermodynamically favored over that of a chlorovinyl species. This result has important implications for the mechanism of dehalogenation of chloroalkenes catalyzed by vitamin B_{12} because it has been shown computationally for the parent cobalt−corrin complex[10] that the corresponding chloroalkylcobalt species, once formed, can decompose rapidly, yielding the dehalogenated olefins. Our results provide additional support that it is indeed this route that is followed in the catalytic cycle of this important process, rather than that via vinylcobalt complexes that had been suggested previously.

Acknowledgment. This work was supported by the Deutsche Forschungsgemeinschaft. M.B. thanks Prof. Walter Thiel and the Max-Planck society for support. Computations were performed on Compaq XP1000, ES40, and Intel Xeon workstations and PCs at the MPI Mülheim and on an IBM p690 cluster at Rechenzentrum Garching, where technical support by H. Lenk and I. Weidl is gratefully acknowledged.

Supporting Information Available: Plots of $\langle f(\xi) \rangle$ values used to construct the ΔA profiles in Figures 4 and 5. This material is available free of charge via the Internet at http://pubs.acs.org.

OM7007474